

## Test of the Gravitational Inverse Square Law at Millimeter Ranges

Shan-Qing Yang, Bi-Fu Zhan, Qing-Lan Wang, Cheng-Gang Shao, Liang-Cheng Tu, Wen-Hai Tan, and Jun Luo\*

*School of Physics, Huazhong University of Science and Technology, Wuhan 430074, People's Republic of China*

(Received 10 December 2011; published 23 February 2012)

We report a new test of the gravitational inverse square law at millimeter ranges by using a dual-modulation torsion pendulum. An I-shaped symmetric pendulum and I-shaped symmetric attractors were adopted to realize a null experimental design. The non-Newtonian force between two macroscopic tungsten plates is measured at separations ranging down to 0.4 mm, and the validity of the null experimental design was checked by non-null Newtonian gravity measurements. We find no deviations from the Newtonian inverse square law with 95% confidence level, and this work establishes the most stringent constraints on non-Newtonian interaction in the ranges from 0.7 to 5.0 mm, and a factor of 8 improvement is achieved at the length scale of several millimeters.

DOI: 10.1103/PhysRevLett.108.081101

PACS numbers: 04.80.Cc

General relativity and the standard model, describing the fundamental physical laws of nature currently, have both passed all experimental tests to date successfully. However, the two theories are essentially incompatible. Physicists have been devoting an intense effort to find a framework that unifies gravity with the rest of physics. Based on ideas from string or M theory, a number of theoretical speculations are proposed and predict that the gravitational interaction could display fundamentally new behavior in a short-range regime [1–8], i.e., a deviation of the Newtonian  $1/r^2$  law in the mm length scale (Ref. [7] provides a comprehensive review). Therefore, any experimental efforts devoted to validating the expectation will help to understand the fundamental nature of gravity.

A large amount of experimental results [9–17] and ongoing searches [18] for a possible violation of the Newtonian  $1/r^2$  law over short scales had been performed. The Yukawa-type potential due to new interactions is typically used to modify the gravitational inverse square law:

$$V(r) = -G \frac{m_1 m_2}{r} (1 + \alpha e^{-r/\lambda}), \quad (1)$$

where  $\alpha$  and  $\lambda$  are the strength and length scale of a new interaction. Up to now, the best bounds on  $\alpha$  in the ranges from  $0.7 \mu\text{m}$  to several meters were reported by Lamoreaux's group [11], Kapitulnik's group [12], Adelberger's group [14], Newman's group [16], and Paik's group [17]. However, the current bounds for  $0.7 \text{ mm} \leq \lambda \leq 5.0 \text{ mm}$  are not as strong as in other regions, which motivates us to perform the further test of the Newtonian  $1/r^2$  law at separations ranging down to 0.4 mm reported in this Letter.

Generally, a high precision test of the  $1/r^2$  law at millimeter ranges requires the thickness of the test and source masses and the change of the gap between them to be on the order of millimeters, and the area of the masses to be as large as possible to increase the non-Newtonian

signal. This means the compensation of the larger Newtonian force should be more precise compared with that in submillimeter or more smaller ranges. Our tests were made with an upgraded version of the I-shaped pendulum used in our previous work [15]. The pendulum used in this work, shown in Fig. 1, consisted of three rectangular glass blocks with dimensions of  $67.67 \times 16.02 \times 7.90 \text{ mm}^3$  for the middle one and  $16.02 \times 16.02 \times 26.85 \text{ mm}^3$  for the two end ones. Two pure tungsten plates with the same dimensions of  $15.994 \times 15.986 \times 1.787 \text{ mm}^3$ , used as the test mass ( $W_1$ ) and the counterbalance one ( $W_2$ ), were adhered to the two end glass blocks symmetrically. The pendulum with a total mass of 75.410 g was suspended by a 600-mm-long, 25- $\mu\text{m}$ -diameter tungsten fiber.

The source mass platform, facing to the pendulum, was designed to have the same I-shaped structure, which consisted of three rectangular glass blocks with approximately the same sizes as the pendulum's. A larger tungsten source mass ( $W_3$ ) with dimension  $20.804 \times 20.778 \times 1.787 \text{ mm}^3$  was adhered to the end block opposite to the test mass. The non-Newtonian force to be measured is between  $W_1$  and  $W_3$  for separations ranging from 0.4 to 1.0 mm, where the net torque change of the Newtonian force was counteracted by a thicker tungsten counterweight mass ( $W_4$ ) with dimensions of  $15.985 \times 15.900 \times 7.645 \text{ mm}^3$ , adhered on the other end block and located behind  $W_3$  about 4 mm in the  $Z$  direction (as shown in Fig. 1). Because the separations between the compensation blocks is larger than that between the test mass and the source mass, the expected non-Newtonian effect (between  $W_1$  and  $W_3$ ) should not be suppressed. Therefore, the test is a null experiment with respect to the net Newtonian torque on the balance.

In order to realize a null experiment, the tungsten plates and all the glass blocks were carefully ground, polished, and precisely assembled as described in Ref. [15]. Two main improvements were made to achieve a more precise

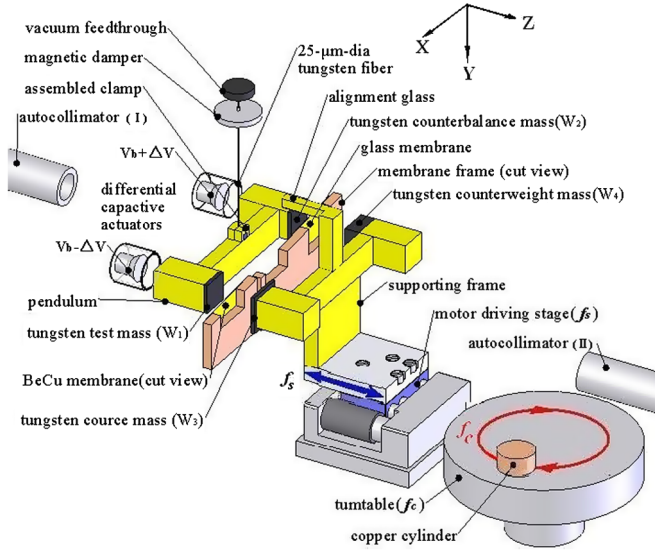


FIG. 1 (color online). Schematic drawing of the experimental setup (not to scale). The membrane frames, the source mass, and its driving stage were mounted on a 6-degree-of-freedom stage (not shown here), which was used to adjust the relative positions and orientation. The protrudent left surface of the alignment glass was used to touch the fiber by moving the source mass in  $X$  direction to acquire the relative positions between the pendulum and the source mass. The pendulum twist was measured by the autocollimator I, and controlled by applying differential voltages to the two capacitive actuators. The separation between the tungsten test and source masses was modulated by driving a motor translation stage with frequency  $f_s$ , and the sensitivity of the pendulum was calibrated by rotating the copper cylinder at frequency  $f_c$ . The autocollimator II was used to monitor the changes of the source mass's attitude synchronously due to the yaw and pitch motions of the driving stage around its shaft.

cancellation of the changes of the Newtonian force. (1) The clamp was assembled by three elaborately ground and polished glass blocks, which helped to locate the suspended fiber to the center of the pendulum's body with an uncertainty of  $1.5 \mu\text{m}$  in the  $X$  direction. (2) An L-shaped glass (the alignment glass in Fig. 1) was used to touch the fiber in the  $X$  direction to acquire the relative positions, and then the source mass can be adjusted face to face with the test mass with an uncertainty of  $1.9 \mu\text{m}$  in the  $X$  direction. By taking the errors of all actual measurements into account, the net change of the Newtonian torque in the experimental range (0.4–1.0 mm) was calculated to be  $\Delta\tau = (0.65 \pm 1.59) \times 10^{-16} \text{ N m}$  (peak-peak), and a perfect cancellation was designed at the gap of 0.7 mm between the test and the source mass. Therefore, the total uncertainty of the amplitude was determined to be  $0.9 (= \frac{1}{2}\sqrt{0.65^2 + 1.59^2}) \times 10^{-16} \text{ N m}$ . The main error budget of the  $\Delta\tau$  is shown in Table I.

Spurious torques from the electrical force between  $W_1$  and  $W_3$  was minimized by inserting a tightly stretched,  $45\text{-}\mu\text{m}$ -thick square beryllium-copper membrane, and the

TABLE I. The main error budget (with  $1\sigma$ ).

Main error sources	Measurement uncertainty	$\delta(\Delta\tau)$ ( $10^{-16} \text{ N m}$ )
Tungsten plate $W_1$		
Thickness	$0.12 \mu\text{m}$	0.24
Mass	$0.6 \text{ mg}$	0.28
Mass of adhesive on $W_1$	$1.0 \text{ mg}$	0.41
Tungsten plate $W_2$		
Thickness	$0.12 \mu\text{m}$	0.27
Mass	$0.6 \text{ mg}$	0.27
Mass of adhesive on $W_2$	$1.0 \text{ mg}$	0.40
Tungsten plate $W_3$		
Thickness	$0.13 \mu\text{m}$	0.30
Position in $Z$ direction	$0.42 \mu\text{m}$	0.26
Mass of adhesive on $W_3$	$1.0 \text{ mg}$	0.40
Tungsten plate $W_4$		
Position in $Z$ direction	$0.38 \mu\text{m}$	0.32
Density inhomogeneity		0.42
Position of fiber in $X$ direction	$1.47 \mu\text{m}$	0.44
Alignments <sup>a</sup>		0.76
Stability of PI driving stage		0.28
Others <sup>b</sup>		0.69
Total		1.59

<sup>a</sup>Relative positions and parallels between the pendulum and source mass platform.

<sup>b</sup>Total uncertainties of dimensions and positions of the glass blocks and other tiny error sources.

smallest gap between  $W_1$  and the membrane was set to  $(263 \pm 1) \mu\text{m}$ . For the same reason, a  $200\text{-}\mu\text{m}$ -thick glass membrane was inserted between  $W_2$  and  $W_4$ , and a larger gap between the  $W_2$  and the membrane was kept to about  $2.7 \text{ mm}$ . The pendulum, the glass blocks, and the membranes were all gold-coated to lower the effect of the electrostatic interactions. Furthermore, to further minimize the difference of the electrostatic surface potential, the residual differential potential between the pendulum and the two membranes were found, respectively, and then compensated individually in each experimental cycle by using the same method as described in Ref. [15].

The entire system was installed inside a vacuum chamber maintained at a pressure of approximately  $10^{-5} \text{ Pa}$  by an ion pump. The torsional motion of the pendulum was monitored by the autocollimator I. The pendulum-to-membrane separation was first set at approximately  $3 \text{ mm}$ , and the free oscillation of the pendulum was recorded. The fiber's torsional spring constant is  $k_f = (8.99 \pm 0.06) \times 10^{-9} \text{ N m/rad}$ , determined from the intrinsic period ( $T_0 = 680.0 \pm 2.0 \text{ s}$ ) and the inertia momentum [ $I_p = (10.54 \pm 0.01) \times 10^{-5} \text{ kg m}^2$ ] of the pendulum. A copper cylinder for gravitational calibration, mounted on a turntable fixed outside of the vacuum chamber, was rotated continuously at a period  $T_{\text{co}} = 400 \text{ s}$ . The response of the pendulum was accordingly determined as  $\tau_{\text{co}} = (5.6 \pm 0.4) \times 10^{-16} \text{ N m}$  (shown in the top panel in

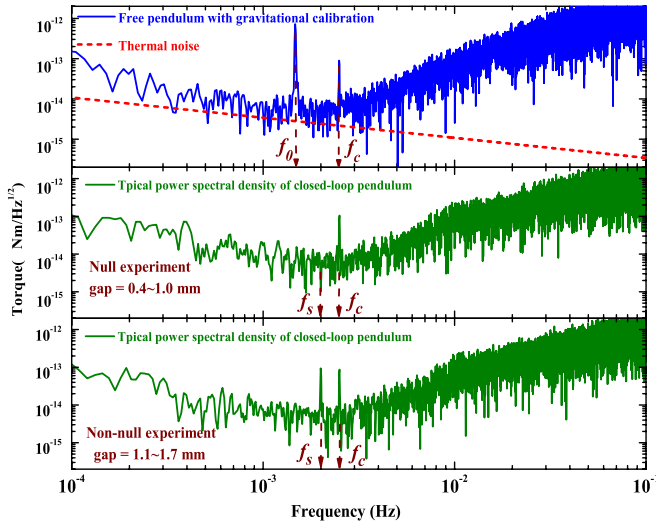


FIG. 2 (color online). The typical PSD of the torque experienced by the open-loop (top panel) and closed-loop (middle and bottom panel) pendulum. The gravitational calibrating signal occurred at  $f_c = 2.5$  mHz in each graph with an amplitude of  $(5.6 \pm 0.4) \times 10^{-16}$  N m. Top panel: The typical PSD curve of the free pendulum with the pendulum-membrane gap being 3 mm. The  $f_0$  ( $= 1.47$  mHz) is the natural frequency of the pendulum. The dash line shows the thermal noise limit inferred from the finite quality factor,  $Q \approx 2000$ . Middle panel: The typical PSD curve of the null experiment with the gap ranging from 0.4 to 1.0 mm, and the expected non-Newtonian signal at  $f_s$  did not appear with the sensitivity of approximately  $0.5 \times 10^{-16}$  N m. Bottom panel: The typical PSD curve of the non-null experiment with the gap ranging from 1.1 to 1.7 mm, and the measured change of the Newtonian torque at  $f_s = 2.0$  mHz is  $(5.7 \pm 1.0) \times 10^{-16}$  N m, in accord with the theoretical calculation of  $(5.5 \pm 0.8) \times 10^{-16}$  N m.

Fig. 2), which was constant and hence used to diagnose the sensitivity of the closed-loop pendulum in subsequent measurements.

The motion of the pendulum was controlled by using a proportional-integral-differential feedback system [15]. In this case, the tungsten fiber was always untwisted during the measurement and the feedback voltage  $\Delta V$  reflected the changes of all effective torques experienced by the pendulum. The quasistatic pendulum in the closed-loop operation allowed us to achieve a small separation ( $263 \pm 1 \mu\text{m}$ ) between the test mass and the beryllium-copper membrane due to the stable electrostatic force between them.

The motor translation stage was then operated continuously with the displacement of a sinusoidal function of time at a frequency  $f_s$  to move the source mass backwards and forwards in a range of 0.6 mm. Meanwhile, the copper cylinder outside for the gravitational calibration was also rotating synchronously with a frequency  $f_c$ . We reduced the  $1/f$  torque noise by increasing the frequencies of the dual modulations to  $f_s = 2.0$  mHz and  $f_c = 2.5$  mHz,

larger than that used in our previous test [15] with  $f_s = 0.463$  mHz and  $f_c = 0.556$  mHz, respectively.

The recorded data, including the outputs of the two autocollimators, the feedback voltage  $\Delta V$ , four temperature sensors, and one barometer, were collected continuously at a sampling rate of 1 Hz with a duration time of approximately 1 day. To extract the expected signal, four main steps were performed as follows: (1) Each data run was broken into separate ‘‘cuts’’ containing exactly the lowest common multiple of the dual-modulation periods of 2000 s. For each ‘‘cut,’’ the feedback voltage  $\Delta V$  at frequency  $f$  ( $f = f_s, f_c$ ) was fitted with

$$\Delta V(t) = a_c \cos(2\pi f_c t) + b_c \sin(2\pi f_c t) + a_s \cos(2\pi f_s t) + b_s \sin(2\pi f_s t) + \sum_{n=1}^2 c_n P_n, \quad (2)$$

where the  $c_n$  coefficients of the Legendre polynomials  $P_n$  accounted for a continuous creeping of the tungsten fiber. The amplitude of the calibration signal at  $f_c$  was  $\Delta V_c = \sqrt{a_c^2 + b_c^2}$ , and hence the calibrated coefficient of  $\beta = \tau_{co}/\Delta V_c$  could be determined, where  $\tau_{co} = (5.6 \pm 0.4) \times 10^{-16}$  N m with an initial phase of zero, and the phase lag was not observed in the pendulum under an accuracy of 0.08 rad. So, the amplitude of the expected torque signal at  $f_s$  was  $\Delta \tau_s = \gamma \beta \sqrt{a_s^2 + b_s^2}$ , where  $\gamma$  [with an amplitude of 1.05(2) and a phase angle of 0.03(2) rad, respectively] accounted for the ratio of the transfer function of the closed-loop performance at  $f_c$  and  $f_s$ . (2) Care was taken to minimize the electromagnet couplings of the motor translation stage, which changed the stable electrostatic field between the pendulum and the shielding membrane periodically due to the variation magnetic field deduced from the running of the motor, and thus contributed a spurious signal at  $f_s$ . To distinguish the spurious effect, we performed an additional background measurement with the source mass platform removed from the motor stage. By only running the stage backwards and forwards with a frequency of  $f_s$  for the same range, an obvious net torque signal was found. After being shielded by two layers of cobalt-based amorphous magnetic shielding films around the motor, the net torque was minimized to be  $a_{sm} = (-1.0 \pm 0.3) \times 10^{-16}$  N m and  $b_{sm} = (1.0 \pm 0.2) \times 10^{-16}$  N m, which, as a bias, could be subtracted in the signals measured with the source mass being on the stage as the same phase. (3) During the running of the translation stage, the typical attitude change of the source mass platform around the  $Y$  axis at  $f_s$  was  $(0.49 \pm 0.05) \mu\text{rad}$  in the cosine component and  $(3.05 \pm 0.03) \mu\text{rad}$  in the sine one, determined from the data monitored synchronously by the autocollimator II. And, the resultant torque signal was  $a_{s\theta} = (0.43 \pm 0.04) \times 10^{-16}$  N m and  $b_{s\theta} = (2.68 \pm 0.03) \times 10^{-16}$  N m, respectively, which could be corrected. (4) Nongravitational backgrounds from the temperature variation, the magnetic,

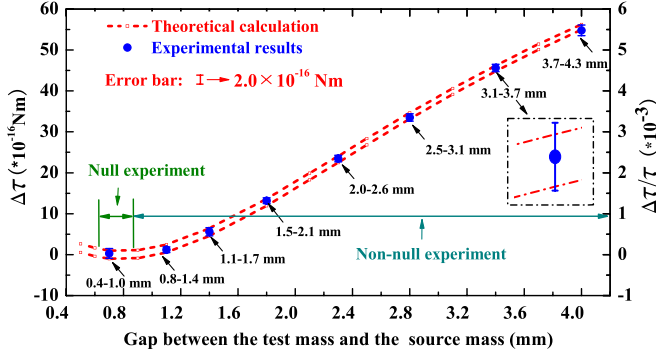


FIG. 3 (color online). Comparison of the change of the Newtonian torque ( $\Delta\tau$ ) between the theoretical calculations (dash) and the experimental results (dot) in each 0.6 mm-range experiment. The gap between the two dashes shows an uncertainty of less than  $2 \times 10^{-16}$  N m, yielded by the dimension errors of the apparatus. The  $\tau$  ( $\sim 1 \times 10^{-12}$  N m), accounting for the net Newtonian torque between the pendulum and the source mass platform, is a constant on the lever of 3% in the total experimental region (0.4–4.3 mm), and a perfect cancellation of it was designed at the gap of 0.7 mm. The inset is a magnified view of the result obtained in 3.1–3.7 mm.

and the air pressure, were studied and found to be negligible using techniques described in Ref. [15].

For 11 data sets (approximately 430 cuts) with the gap ranging from 0.4 to 1.0 mm, the mean amplitude of the expected torque at  $f = f_s$  was yielded as

$$\Delta\tau_s = (0.4 \pm 0.9_{\text{stat}} \pm 0.9_{\text{sys}}) \times 10^{-16} \text{ N m}, \quad (3)$$

where the first uncertainty is statistic, and the second is systematic uncertainty induced from the Newtonian gravitation compensation. It means that no violation of the Newtonian  $1/r^2$  law is observed at the present experimental ranges in the level of the pendulum's sensitivity. A typical power spectral density (PSD) curve is shown in Fig. 2 (in the middle panel). In order to check the validity of the null experiment design, the non-null experiment was performed by extending the separation between the test mass and the source mass, where the obvious net Newtonian torque allows precision measurements with the same procedure. By varying the gap at 0.8–1.4 mm, 1.1–1.7 mm, ..., and 3.7–4.3 mm, respectively, (as shown in Fig. 3), some non-null test were done, and a typical PSD curve of the torque experienced by the closed-loop pendulum with the gap ranging from 1.1 to 1.7 mm is shown in the bottom panel in Fig. 2. The total experiment results show a perfect consistence with the theoretical calculations of the change of the Newtonian torque (shown in Fig. 3), which provide an additional check to the total experimental system, and hence further enhance the null experiment's confidence.

The total uncertainty of the torque noise is computed to be  $\Delta\tau_s \leq 1.3 \times 10^{-16}$  N m, and we used  $2\Delta\tau_s$  to set constraints on the additional Yukawa interaction according to

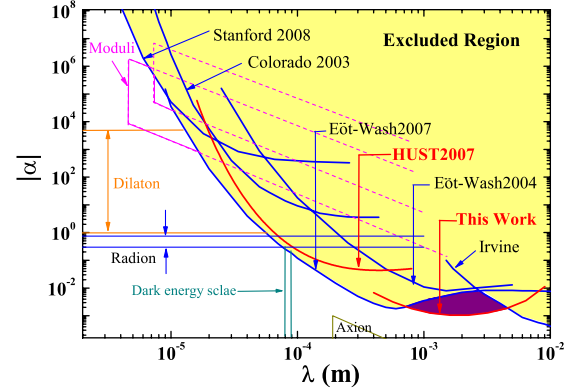


FIG. 4 (color online). Upper limits on Yukawa violations of the Newtonian  $1/r^2$  law. The shaded region is excluded with 95% confidence level. The heavy lines labeled Stanford 2008 [12], Colorado 2003 [13], Eöt-wash 2004 and 2007 [14], HUST 2007 [15], This work, and Irvine [16] show the experimental constraints, respectively. Lighter lines showed various theoretical predictions summarized in [7].

Eq. (1). We establish the new best constraints on non-Newtonian interaction in the ranges from 0.7 to 5.0 mm under 95% confidence level, shown in Fig. 4. At the length scale of several millimeters, we improve the previous bounds by up to a factor of 8, and find no deviations from the Newtonian  $1/r^2$  law. The present sensitivity was basically limited by the compensation of the Newtonian force. Aiming to explore some new phenomena of gravitation at an even shorter range, we are preparing an improved experiment in the submillimeter length scale with higher precisions, and looking forward to getting some new results in the near future.

We are very appreciative of Riley Newman, Ho Jung Paik, and Vadim Milyukov for their helpful suggestions and discussion. This work was supported by the National Basic Research Program of China under Grant No. 2010CB832802.

\*junluo@mail.hust.edu.cn

- [1] N. Arkani-Hamed, S. Dimopoulos, and G. Dvali, *Phys. Lett. B* **429**, 263 (1998); *Phys. Rev. D* **59**, 086004 (1999).
- [2] N. Arkani-Hamed, S. Dimopoulos, G. Dvali, and N. Kaloper, *Phys. Rev. Lett.* **84**, 586 (2000).
- [3] S. Dimopoulos and G. F. Giudice, *Phys. Lett. B* **379**, 105 (1996).
- [4] R. Sundrum, *J. High Energy Phys.* 07 (1999) 001; *Phys. Rev. D* **69**, 044014 (2004).
- [5] L. Randall and R. Sundrum, *Phys. Rev. Lett.* **83**, 4690 (1999).
- [6] D. B. Kaplan and M. B. Wise, *J. High Energy Phys.* 08 (2000) 037.
- [7] E. G. Adelberger, B. R. Heckel, and A. E. Nelson, *Annu. Rev. Nucl. Part. Sci.* **53**, 77 (2003).
- [8] E. G. Adelberger *et al.*, *Phys. Rev. Lett.* **98**, 131104 (2007).

- [9] R. S. Decca *et al.*, *Phys. Rev. Lett.* **94**, 240401 (2005).
- [10] M. Masuda and M. Sasaki, *Phys. Rev. Lett.* **102**, 171101 (2009).
- [11] S. K. Lamoreaux, *Phys. Rev. Lett.* **78**, 5 (1997); A. O. Sushkov, W. J. Kim, D. A. R. Dalvit, and S. K. Lamoreaux, *ibid.* **107**, 171101 (2011).
- [12] J. Chiaverini *et al.*, *Phys. Rev. Lett.* **90**, 151101 (2003); A. A. Geraci *et al.*, *Phys. Rev. D* **78**, 022002 (2008).
- [13] J. C. Long *et al.*, *Nature (London)* **421**, 922 (2003).
- [14] C. D. Hoyle *et al.*, *Phys. Rev. D* **70**, 042004 (2004); D. J. Kapner *et al.*, *Phys. Rev. Lett.* **98**, 021101 (2007).
- [15] L. C. Tu *et al.*, *Phys. Rev. Lett.* **98**, 201101 (2007).
- [16] J. K. Hoskins, R. D. Newman, R. Spero, and J. Schultz, *Phys. Rev. D* **32**, 3084 (1985).
- [17] M. V. Moody and H. J. Paik, *Phys. Rev. Lett.* **70**, 1195 (1993).
- [18] R. D. Newman, E. C. Berg, and P. E. Boynton, *Space Sci. Rev.* **148**, 175 (2009).